

## Effect of hexadecyl trimethyl ammonium bromide on sonocatalytic degradation of Orange II by using bagasse biochar

Guoting Li<sup>a,\*</sup>, Shude Zhang<sup>a</sup>, Panpan Yu<sup>a</sup>, Xiao Mi<sup>a</sup>, Yujie Guo<sup>a</sup>, Chenliang Shen<sup>b</sup>

<sup>a</sup>School of Environmental and Municipal Engineering, North China University of Water Resources and Electric Power, Zhengzhou 450046, China, Tel.: +86-371-69127436; Fax: +86-371-65790239; emails: lipsonny@163.com (G.T. Li), zshude@126.com (S.D. Zhang), ypp9903@163.com (P.P. Yu), mixiao@ncwu.edu.cn (X. Mi), guoyujie@ncwu.edu.cn (Y.J. Guo)

<sup>b</sup>Zhongzhou Water Holding Co., Ltd., Zhengzhou 450046, China, email: shenchenl@126.com (C.L. Shen)

Received 27 June 2023; Accepted 1 October 2023

### ABSTRACT

The heterogeneous micro-interface plays a crucial role in facilitating mass transfer and catalytic conversion. This study aimed to investigate the influence of the surfactant cetyltrimethyl ammonium bromide (CTAB) on micro-interface properties during sonocatalytic degradation of Orange II using bagasse biochar. Our findings indicate that increasing the concentration of CTAB or the dosage of bagasse biochar significantly enhances sonocatalytic degradation efficiency. However, an increase in solution pH was observed to have a detrimental effect on degradation efficiency, while higher ultrasonic power proved beneficial for Orange II degradation when CTAB was present. Moreover, the pseudo-first-order rate constant ( $K_{app}$ ) for the sonocatalytic process was 1.3 times that of the sum of combined  $K_{app}$  values obtained with ultrasonication and biochar adsorption individually, indicating a substantial synergistic effect when bagasse biochar and ultrasonication are combined in the presence of CTAB. The influence of inorganic anions on sonocatalytic degradation of Orange II, in the presence of CTAB, was relatively weak. Quenching tests using iso-propanol and KBr indicated that free radical chain reactions predominantly occurred at the micro-interface, with limited involvement in bulk solutions during the sonocatalytic degradation process. Overall, our results indicate that OH radicals remained the dominant contributors to the overall reaction.

**Keywords:** Cetyltrimethyl ammonium bromide (CTAB); Orange II; Interface; Bagasse biochar; Sonocatalytic degradation

### 1. Introduction

Advanced oxidation processes (AOPs) are characterized by the generation and utilization of a variety of highly reactive oxidizing species, including non-selective OH radicals, sulfate radicals, and hydrogen peroxide. As a result, AOPs can be considered as destructive technologies since the majority of the targeted organic contaminants are effectively decomposed and even transformed into carbon dioxide, inorganic substances, and water. Numerous organic pollutants have been observed to undergo efficient degradation in aqueous solutions [1–8]. In fact, AOPs

have the capability to break down virtually all types of organic contaminants into non-hazardous substances [2]. One notable AOPs, sonocatalysis, has garnered increasing attention due to its ability to eliminate common environmental contaminants effectively and with simplicity. During sonochemical process, acoustic cavitation generates hot spots with localized temperatures and pressures on the order of 5,000 K and hundreds of atmospheres, respectively. As a result of thermal dissociation of water vapor through a series of reactions, reactive radicals like OH and OOH radicals are formed and actively participate in the

\* Corresponding author.

decomposition of target contaminants [3]. The degradation of contaminants through ultrasound primarily relies on the phenomenon of acoustic cavitation. Additionally, it has been demonstrated that high-frequency ultrasound is effective in breaking down non-polar pollutants, such as hydrocarbons and aromatic contaminants [4,5].

In addition, the incorporation of sonocatalysts is essential to achieve higher degradation efficiency, as the sonochemical process alone exhibits limited efficiency and consumes a significant amount of energy for decontamination. The efficiency of these sonocatalytic processes can be improved dramatically by various catalysts [9–11]. However, many of the sonocatalysts currently under exploration consist of synthesized metal oxides such as  $\text{MnO}_2$  and  $\text{TiO}_2$ . In practice, cost-effective sonocatalysts are favored for potential applications in water and wastewater purification.

Recent advancements suggest that low-cost carbonaceous materials, including waste biomasses and biochars derived from biomass, hold promise as potential catalysts for sonocatalytic degradation processes. While waste biomasses are abundant in natural environments, they are not ideal for sonocatalytic processes due to the potential leaching of organic compounds, which could lead to secondary pollution. In contrast, biochars derived from these biomasses offer a more suitable option, as they are rich in carbon and exhibit stability that prevents organic leaching and secondary pollution. Additionally, biochars with a characteristic mesoporous structure can be easily obtained through incomplete combustion processes like low-temperature pyrolysis and carbonization [12–14]. As such, some of the biochars might be ideal metal-free candidates for sonocatalytic degradation processes. Our previous study was the first to demonstrate that biochar derived from sugarcane bagasse exhibited excellent sonocatalytic activity in the synergistic degradation of methylene blue [15]. Other research has further confirmed the capability of biochar as a sonocatalyst for the oxidation of propylparaben, bisphenol A, and persistent organic contaminants [16–18]. Low-cost biochar has the potential to serve as a cost-effective, metal-free sonocatalyst in practical water and wastewater treatment applications.

Moreover, employing various catalysts in sonocatalytic degradation processes can fundamentally alter the characteristics of the water-catalyst interface. The heterogeneous micro-interface serves as a crucial platform for processes such as adsorption/desorption, flocculation, catalytic conversion, and biotransformation of contaminants [19]. Given the charge and structural properties of contaminants, it is possible to strategically engineer and design the heterogeneous micro-interface to enhance catalytic performance. Amphiphilic surfactants are widely used as surface-active agents for improving the efficiency of various processes [20]. Normally, surfactant cetyltrimethyl ammonium bromide (CTAB) modified adsorbent could significantly improve adsorption capability of adsorbent matrix for the removal of negatively-charged contaminants such as furfural, bisphenol A, methylene blue, Cr(VI), nitrate and phosphate ions [21–23]. Actually, a number of surfactants are existent in industrial effluents, municipal wastewater and even in natural water environments as the conventional bio-treatment methods are not always effective for removing these low-concentration contaminants [20,24]. Direct

introduction of a very limited amount of CTAB into reaction mixture could significantly enhance adsorption of Orange II on bagasse-derived biochar in our finished research [25]. By contrast, it was found by other researchers that the presence of CTAB and sodium dodecylsulfate retarded the persulfate activation and oxidation of Orange II to some extent [26]. From this point of view, the surfactant CTAB is capable of regulating the properties of heterogeneous micro-interface, and thus manipulating the related adsorption and catalytic performance to some extent.

In this study, we introduced an innovative approach to control the characteristics of the heterogeneous micro-interface *in-situ*. This approach involved the direct introduction of a minimal amount of the surfactant CTAB into the aqueous solution. The result was an enhanced sonocatalytic degradation capacity of bagasse biochar for the removal of Orange II. We investigated various factors, including CTAB concentration in the solution, biochar dosage, solution pH, ultrasonic power, and their synergistic effects, to assess their impact on the process. Furthermore, we evaluated the oxidation mechanism by conducting indirect quenching tests using iso-propanol and KBr.

## 2. Materials and methods

### 2.1. Materials

Orange II (ORII) and CTAB were obtained from Beijing Chemical Reagents Company and utilized without undergoing additional purification. All other chemicals employed in the study were of analytical grade. Deionized (DI) water was consistently used throughout the entire investigation.

### 2.2. Preparation of sugarcane bagasse biochar

Sugarcane bagasse was collected from Guangxi Province of China. It was washed, dried, crushed and sieved using a 100-mesh sieve. The bagasse biochars were prepared via pyrolyzing the bagasse biomass at 600°C under oxygen-limited conditions for 2 h. The detailed procedures for the preparation of the bagasse biochar can be referred to our previous study [27].

### 2.3. Sonocatalytic degradation of ORII in the presence and absence of CTAB

Sonocatalytic degradation of Orange II by using bagasse biochar in the presence and absence of CTAB was carried out in a series of cylindrical flasks for 60 min. The available volume of the flasks was 250 and 200 mL of ORII solution (5 mg/L) was added. Sonication was performed in a 40 kHz ultrasonic cleaning bath (AS3120A, Kunshan Ultrasonic Instruments Co., Jiangsu, China). The power of the ultrasonic cleaning bath was fixed at 50 W unless otherwise stated. The water-circulating unit was used to control water bath temperature. All the solution pH was maintained at neutral pH except for the pH effect study. The solution pH adjustment was conducted by addition of diluted HCl or NaOH solution. In the alcohol quenching test, 0.05 mol/L isopropanol (ISP) was used. For KBr quenching, the dosages of KBr were 0.01, 0.05 and 0.10 mol/L, respectively.

## 2.4. Analyses

Samples were collected and subsequently filtered through a 0.45  $\mu\text{m}$  membrane before analyzing. The concentrations of ORII were determined by measuring the maximum absorbance at a fixed wavelength of 484 nm, using an UVmini-1240 spectrophotometer (Shimadzu, Japan).

The pseudo-first-order kinetics of the degradation processes was simulated as:

$$\ln\left(\frac{C_0}{C_t}\right) = K_{\text{app}} \cdot t \quad (1)$$

where  $C_t$  is the dye concentration at time  $t$  (mg/L),  $C_0$  is the initial dye concentration (mg/L), and  $K_{\text{app}}$  is the apparent first-order rate constant ( $\text{min}^{-1}$ ).

## 3. Results and discussion

### 3.1. Effect of CTAB concentration on sonocatalytic degradation of ORII

Since CTAB has the capability to significantly alter the interface properties and subsequently impact the adsorption of ORII onto bagasse biochar, it was expected that the sonocatalytic degradation performance could be influenced significantly by the introduction of CTAB. The effect of CTAB concentration on sonocatalytic degradation of ORII was examined and is illustrated in Fig. 1. The CTAB concentration ranged from 0 to 6.0 mg/L. Through pseudo-first-order kinetic simulation, the  $K_{\text{app}}$  values determined at the CTAB concentration of 0, 0.5, 1.0, 2.0, 4.0 and 6.0 mg/L were of 0.00373, 0.00507, 0.00589, 0.00855, 0.01521 and 0.04265  $\text{min}^{-1}$  ( $R^2 = 0.937, 0.920, 0.890, 0.999, 0.968$  and  $0.973$ ), respectively. It is evident that the presence of 6.0 mg/L CTAB could enhance the  $K_{\text{app}}$  value by up to ten times when compared to the  $K_{\text{app}}$  value in the absence of CTAB. Clearly, an increased CTAB concentration had a beneficial effect on the sonocatalytic degradation of ORII. Considering potential adverse effects of higher CTAB concentrations, we selected 2.0 mg/L as the fixed CTAB concentration for subsequent tests.

### 3.2. Effect of biochar dosage on sonocatalytic degradation of ORII

The effect of bagasse biochar dosage on the sonocatalytic degradation of ORII was also investigated in the presence of 2.0 mg/L CTAB, as illustrated in Fig. 2. The biochar dosages of 50, 100, 150, 200 and 300 mg in 200 mL of solution were selected. It can be observed that the  $K_{\text{app}}$  values at the dosages of 50, 100, 150, 200 and 300 mg were of 0.00424, 0.00526, 0.00855, 0.00990 and 0.01099  $\text{min}^{-1}$  ( $R^2 = 0.998, 0.992, 0.999, 0.996$  and  $0.995$ ), respectively. The increased catalyst dosage could increase the available active sites of bagasse biochar for adsorption and catalytic oxidation. Consequently, the sonocatalytic degradation efficiency improved with a higher dosage of biochar, although the  $K_{\text{app}}$  values did not exhibit as substantial an enhancement as observed with the CTAB concentration effect. In comparison to a biochar dosage of 150 mg, the  $K_{\text{app}}$  value at a dosage of 200 mg did not exhibit a significant increase, leading us to select 150 mg as the fixed biochar dosage for the subsequent tests.

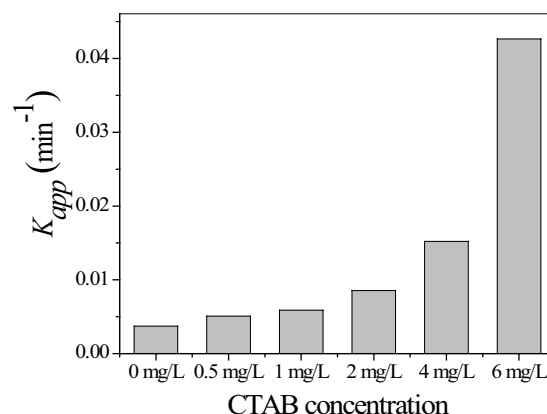


Fig. 1. Effect of CTAB concentration on sonocatalytic degradation of ORII. Biochar dose 150 mg, at neutral solution pH.

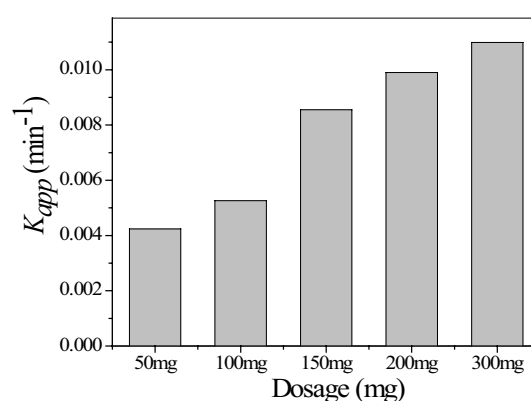


Fig. 2. Effect of bagasse biochar dosage on sonocatalytic degradation of ORII. CTAB concentration 2.0 mg/L, neutral solution pH.

### 3.3. Effect of solution pH on sonocatalytic degradation of ORII

Both surfactant CTAB and solution pH could influence the interface property and interaction between biochar and ORII molecules profoundly. As such, the effect of solution pH on the sonocatalytic degradation of ORII was investigated from pH 3.0 to pH 11.0 in the presence of 2.0 mg/L CTAB. As illustrated in Fig. 3, the  $K_{\text{app}}$  values at pH 3.0, 5.0, 7.0, 9.0 and 11.0 were of 0.01015, 0.00968, 0.00855, 0.00674 and 0.00577  $\text{min}^{-1}$  ( $R^2 = 0.984, 0.982, 0.999, 0.979$  and  $0.990$ ), respectively. Evidently, acidic conditions were favorable for ORII removal and the sonocatalytic degradation efficiency declined with increasing solution pH. For ORII molecule,  $\text{p}K_{\text{a}1}$  value for the deprotonation of the naphthalene OH is 11.4 and  $\text{p}K_{\text{a}2}$  value for the deprotonation of  $\text{SO}_3\text{H}$  group is  $\sim 1$  [28]. ORII molecules are negatively charged at almost all the pH range studied. In contrast, the surface of bagasse biochar becomes increasingly negatively charged as the solution's pH rises, even in the presence of CTAB. This heightened negative charge results in a stronger electrostatic repulsion force between the biochar and ORII molecules as the solution's pH increases. Consequently, this leads to a reduced uptake of ORII on the biochar. Given that the adsorption of ORII on the

biochar serves as the initial and crucial step in the sonocatalytic degradation process, the diminished uptake of ORII results in subsequently reduced degradation efficiency.

### 3.4. Effect of ultrasonic power on sonocatalytic degradation of ORII

The effect of ultrasonic power was investigated at in the presence of 2.0 mg/L of CTAB. The ultrasonic power of 50, 80 and 100 W was selected. As presented in Fig. 4, the  $K_{app}$  values at ultrasonic power 50, 80 and 100 W were of 0.00855, 0.00992 and 0.01263  $\text{min}^{-1}$  ( $R^2 = 0.999, 0.996$  and  $0.993$ ), respectively. As increasing ultrasonic power could increase the energy of cavitation while lower the threshold of cavitation, the quantity of cavitation bubbles generated was enhanced accordingly [29]. Because the free radical chain reaction occurs predominately in the interfacial region of the bubbles [15], it was deduced that more free radicals (reactive oxidizing species) were generated concurrently, which contributed to the sonocatalytic degradation of ORII.

### 3.5. Synergetic effect during the combined degradation process

Our previous study has proved the combination of bagasse biochar and ultrasonication led to significant

synergetic effect [15]. In the presence of CTAB, the synergetic effect was also investigated and is presented in Fig. 5. The  $K_{app}$  values by ultrasonication (US) alone, bagasse biochar adsorption alone, and US/biochar combination were of 0.00129, 0.00529, and 0.00855  $\text{min}^{-1}$  ( $R^2 = 0.999, 0.996$  and  $0.993$ ), respectively. The  $K_{app}$  value of the combined process was 1.3 times that of the sum of  $K_{app}$  values of the other two processes. This indicated that an apparent synergetic effect was still observed for the combination of bagasse biochar and ultrasonication in the presence of CTAB.

### 3.6. Effect of salt on sonocatalytic degradation of ORII

The addition of inorganic salts could lead to decrease in the surface tension and critical micellar concentration of micelles forming surfactant, and thus affects the degradation efficiency consequently. In the presence of 2.0 mg/L CTAB, the effect of salt on sonocatalytic degradation of ORII was investigated by adding  $\text{Na}_2\text{SO}_4$ , NaCl and  $\text{NaNO}_3$  with a concentration of 0.01 mol/L. From Fig. 6, the  $K_{app}$  values in the presence of  $\text{Na}_2\text{SO}_4$ , NaCl and  $\text{NaNO}_3$  were of 0.00837, 0.00820, and 0.00846  $\text{min}^{-1}$  ( $R^2 = 0.996, 0.997$  and  $0.996$ ), respectively. Apparently, the presence of these salts had a weak inhibiting effect on the sonocatalytic degradation

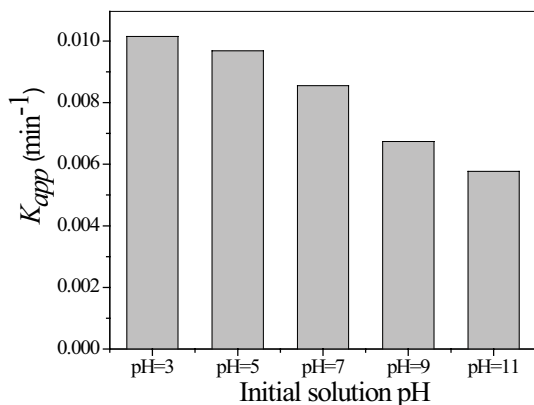


Fig. 3. Effect of solution pH on sonocatalytic degradation of ORII. Biochar dose 150 mg, CTAB concentration 2.0 mg/L.

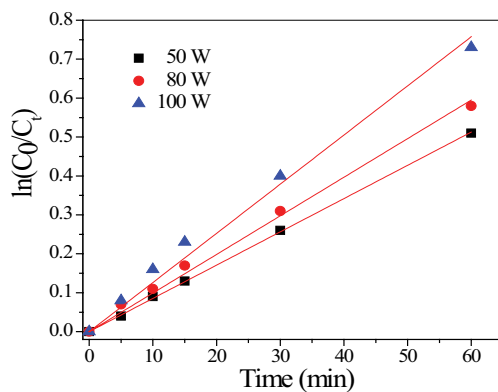


Fig. 4. Effect of ultrasonic power on sonocatalytic degradation of ORII. Biochar dose 150 mg, CTAB concentration 2.0 mg/L, neutral solution pH.

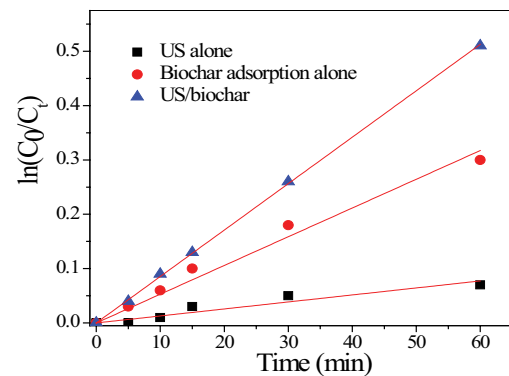


Fig. 5. Pseudo-first-order degradation of ORII by ultrasonication (US) alone, bagasse biochar adsorption alone, and US/biochar combination. Biochar dose 150 mg, CTAB concentration 2.0 mg/L, neutral solution pH.

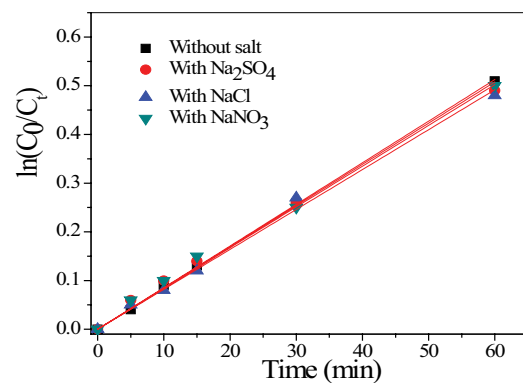


Fig. 6. Effect of salt on sonocatalytic degradation of ORII. Biochar dose 150 mg, CTAB concentration 2.0 mg/L, neutral solution pH.

of ORII in the presence of CTAB. Concerning the salting out effect, more ORII molecules moved to the interface of the cavities and the possibility of radicals attack increased accordingly [30]. On the other hand, these anions including  $\text{SO}_4^{2-}$ ,  $\text{Cl}^-$ , and chloride and  $\text{NO}_3^-$  were expected to quench hydroxyl radicals according to the following equations [31]:



While OH radicals were undeniably generated and played a role in the sonocatalytic degradation of ORII, it was reasonable to anticipate that these anions might have partially quenched the chain reaction of OH radicals, potentially reducing the degradation efficiency. However, it is noteworthy that both the presence of salts had an impact on the degradation of ORII, but their influence was observed to be negligible in this context.

### 3.7. Reaction mechanism

Radicals, especially OH radicals, play an important role during sonocatalytic degradation process. Indirect quenching method by ISP and KBr can be employed to indicate the oxidation mechanism. The inhibitive effect of ISP and KBr on the oxidation process can be quantitatively indicated by the decline in reaction rate constants ( $K_{app}$ ). For one thing, the role of OH radicals was evaluated by isopropanol quenching method. Alcohols such as isopropanol could scavenge OH radicals and were often used to estimate the role of OH radicals [32,33]. The effect of isopropanol (ISP) on sonocatalytic degradation of ORII was presented in Fig. 7a. By ISP (0.05 mol/L) quenching, the  $K_{app}$  values decreased from  $0.00855 \text{ min}^{-1}$  ( $R^2 = 0.993$ ) in the absence of ISP to  $0.00702 \text{ min}^{-1}$  ( $R^2 = 0.999$ ) in the presence of ISP. This implied that the contribution of OH radicals amounted to only 17.9% for the total reaction, which was not as significant as expected in other sonocatalytic processes. For the other thing, KBr was known as a non-volatile scavenger which could be readily oxidized by free radicals [34,35]. The effect of KBr on sonocatalytic degradation of ORII was also investigated and the results were presented in Fig. 7b. The dosage of KBr ranged from 0.01 to 0.10 mol/L. With increasing KBr dosage, the  $K_{app}$  values decreased from  $0.00855 \text{ min}^{-1}$  ( $R^2 = 0.993$ ) in the absence of KBr to  $0.00655 \text{ min}^{-1}$  ( $R^2 = 0.956$ ) in the presence of 0.10 mol/L of KBr. It can be deduced that the contribution of free radicals amounts to only 23.4% for the total reaction.

As a comparison, alcohol including ISP was a known OH radical scavenger for the gaseous region and/or interfacial region of the collapsing bubble. However, differently, KBr was known as a non-volatile scavenger to quench free radicals originated from the bulk liquid region and possibly from the interfacial region of the cavitation bubble [36,37]. Consequently, the contribution percentage of hydroxyl radicals, and free radicals from the bulk liquid region and possibly from the interfacial region reached 17.9% and 23.4% to

the total degradative capability, respectively. As a result, it indicated the free radical chain reactions occurred predominantly within the interfacial region and to a lesser extent in bulk solutions in the sonocatalytic degradation process.

Meanwhile, as almost all the free radicals could be quenched by KBr, it can be deduced that the contribution of other radicals was calculated to be only 5.6% in this case if the contribution of OH radicals was excluded. As such, compared to other free radicals or oxidizing species, the role of OH radicals was still dominant in this process, although other processes such as pyrolytic degradation were still supposed to be capable of degrading ORII efficiently. Other researches also demonstrate that OH radicals play the dominant role in biochar-based sonocatalytic process, although the oxidizing species including OH radicals, superoxide radicals ( $\text{O}_2^{\bullet-}$ ) and  $\text{H}_2\text{O}_2$  are all involved in the degradation process [38]. The scheme for the sonocatalytic degradation of ORII by using bagasse biochar in the presence of CTAB is presented in Fig. 8. Generally, CTAB acts as an electrolyte at lower concentration and ionized in  $\text{CTA}^+$  and  $\text{Br}^-$ , and  $\text{CTA}^+$  forms complex on the surface of bagasse biochar [32]. Consequently, in the initial stage, the water/biochar interface tends to become positively charged. Subsequently, the negatively charged ORII molecules migrate from the bulk solution to the biochar interface, resulting in an increased adsorption of ORII molecules on the positively charged biochar interface. Finally, as the generation and utilization of oxidizing species, particularly OH radicals, predominantly take place at the biochar interface, the intensified adsorption

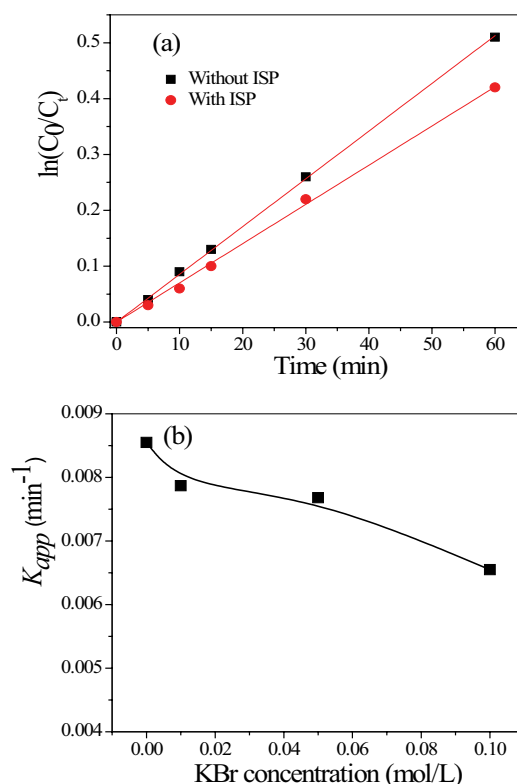


Fig. 7. Effect of iso-propanol (ISP) (a) and KBr (b) on sonocatalytic degradation of ORII. Biochar dose 150 mg, ISP dosage 0.05 mol/L, CTAB concentration 2.0 mg/L, neutral solution pH.



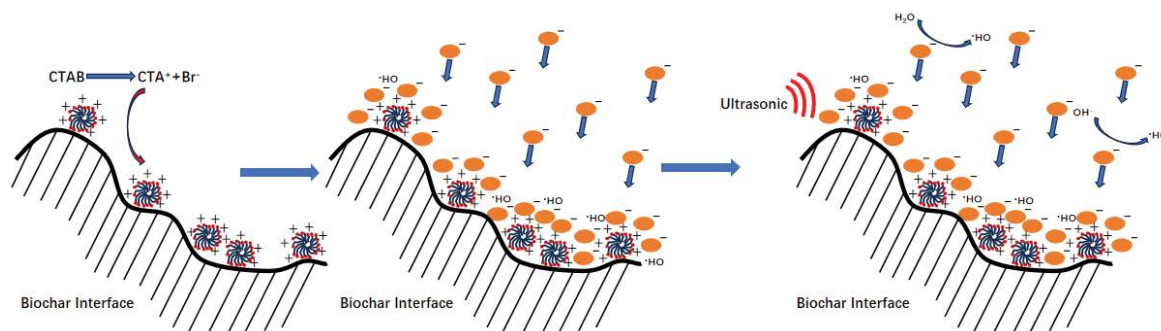


Fig. 8. Mechanism for sonocatalytic degradation of ORII by using bagasse biochar in the presence of CTAB.

of ORII molecules on the biochar interface effectively accelerates the oxidation of ORII molecules and the utilization of oxidizing species in the third stage.

### 3.8. FTIR analysis

FTIR spectra of raw bagasse biochar, bagasse biochar alone after sonocatalytic degradation and bagasse biochar after sonocatalytic degradation in the presence of CTAB were recorded, as shown in Fig. 9. As presented in our previous study [15], the strong band at  $3,439\text{ cm}^{-1}$  represents the stretching vibrations of hydroxyl groups on the bagasse biochar. The bands at  $2,885$  and  $2,920\text{ cm}^{-1}$  are attributed to the asymmetric and symmetric stretching vibrations of aliphatic  $-\text{CH}_2$  in CTAB, respectively [39,40]. The band at  $1,030\text{ cm}^{-1}$  corresponds to C–O–C vibrations. The intensities and locations of these bands are quite constant among the three samples. This indicated these functional groups and biochar surface properties were quite stable which facilitated the sonocatalytic degradation of ORII. Although the band at  $2960\text{ cm}^{-1}$  is unique to CTAB, which corresponds to both trimethyl head group and the terminal methyl of CTAB, there was no obvious absorption at this band for the three samples [41,42].

## 4. Conclusion

The introduction of the surfactant CTAB had a profound impact on the micro-interface between the Orange II solution and bagasse biochar. Higher concentrations of CTAB or increased amounts of bagasse biochar significantly enhanced the efficiency of sonocatalytic degradation. However, in the presence of CTAB, a decrease in sonocatalytic degradation efficiency was observed as the solution pH increased, while an increase in ultrasonic power was found to be beneficial for Orange II degradation. Notably, a pronounced synergistic effect emerged when combining bagasse biochar and ultrasonication in the presence of CTAB. The presence of inorganic anions weakly inhibited the sonocatalytic degradation of Orange II in the presence of CTAB. Quenching tests using iso-propanol and KBr indicated that free radical chain reactions primarily occurred within the interfacial region and to a lesser extent in the bulk solution during the sonocatalytic degradation process. The contribution of OH radicals remained dominant for the overall reaction.

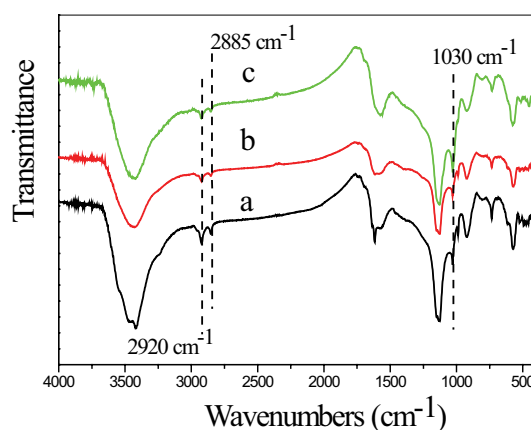


Fig. 9. FTIR spectra of raw bagasse biochar (a), bagasse biochar alone after sonocatalytic degradation (b) and bagasse biochar after sonocatalytic degradation in the presence of CTAB (c).

## Acknowledgement

The Authors thank for financial support from the grant Advanced manufacturing of biochar in UK/China/Malaysia/Nigeria (British Council, UK-China-BRI Countries Education Partnership Initiative, 2019), the National Natural Science Foundation of China (Grant No. 51378205), and the Key research & development and promotion projects in Henan Province (232102321029).

## References

- [1] M. Cocha, G. Farinelli, A. Tiraferri, M. Minella, D. Vione, Advanced oxidation processes in the removal of organic substances from produced water: potential, configurations, and research needs, *Chem. Eng. J.*, 414 (2021) 128668, doi: 10.1016/j.cej.2021.128668.
- [2] S. Esplugas, P.L. Yue, M.I. Pervez, Degradation of 4-chlorophenol by photolytic oxidation, *Water Res.*, 28 (1994) 1323–1328.
- [3] I. Gasmi, O. Hamdaoui, H. Ferkous, A. Alghyamah, Sonochemical advanced oxidation process for the degradation of furosemide in water: effects of sonication's conditions and scavengers, *Ultrason. Sonochem.*, 95 (2023) 106361, doi: 10.1016/j.ultsonch.2023.106361.
- [4] J. Peller, O. Wiest, P.V. Ka, Synergy of combining sonolysis and photocatalysis in the degradation and mineralization of chlorinated aromatic compounds, *Environ. Sci. Technol.*, 37 (2003) 1926–1932.

- [5] Z.H. Diao, F.X. Dong, L. Yan, Z.L. Chen, W. Qian, L.J. Kong, Z.W. Zhang, T. Zhang, X.Q. Tao, J.J. Du, D. Jiang, W. Chu, Synergistic oxidation of Bisphenol A in a heterogeneous ultrasound-enhanced sludge biochar catalyst/persulfate process: reactivity and mechanism, *J. Hazard. Mater.*, 384 (2020) 121385, doi: 10.1016/j.jhazmat.2019.121385.
- [6] D.S. Ma, H. Yi, C. Lai, X.G. Liu, X.Q. Huo, Z.W. An, L. Li, Y.K. Fu, B.S. Li, M.M. Zhang, L. Qin, S.Y. Liu, L. Yang, Critical review of advanced oxidation processes in organic wastewater treatment, *Chemosphere*, 275 (2021) 130104, doi: 10.1016/j.chemosphere.2021.130104.
- [7] D.B. Miklos, C. Remy, M. Jekel, K.G. Linden, J.E. Drewes, U. Hübner, Evaluation of advanced oxidation processes for water and wastewater treatment - a critical review, *Water Res.*, 139 (2018) 118–131.
- [8] A.P. Bhat, P.R. Gogate, Degradation of nitrogen-containing hazardous compounds using advanced oxidation processes: a review on aliphatic and aromatic amines, dyes, and pesticides, *J. Hazard. Mater.*, 403 (2021) 123657, doi: 10.1016/j.jhazmat.2020.123657.
- [9] H. Harada, Sonophotocatalytic decomposition of water using TiO<sub>2</sub> photocatalyst, *Ultrason. Sonochem.*, 8 (2001) 55–58.
- [10] H. Zhao, G.M. Zhang, Q.L. Zhang, MnO<sub>2</sub>/CeO<sub>2</sub> for catalytic ultrasonic degradation of methyl orange, *Ultrason. Sonochem.*, 21 (2014) 991–996.
- [11] N. Ertugay, F.N. Acar, The degradation of Direct Blue 71 by sono, photo and sonophotocatalytic oxidation in the presence of ZnO nanocatalyst, *Appl. Surf. Sci.*, 318 (2014) 121–126.
- [12] Z.H. Zheng, B.L. Zhao, Y.P. Guo, Y.J. Guo, T. Pak, G.T. Li, Preparation of mesoporous batatas biochar via soft-template method for high efficiency removal of tetracycline, *Sci. Total Environ.*, 787 (2021) 147397, doi: 10.1016/j.scitotenv.2021.147397.
- [13] W.S. Chen, B.L. Zhao, Y.P. Guo, Y.J. Guo, Z.H. Zheng, T. Pak, G.T. Li, Effect of hydrothermal pretreatment on pyrolyzed sludge biochars for tetracycline adsorption, *J. Environ. Chem. Eng.*, 9 (2021) 106557, doi: 10.1016/j.jece.2021.106557.
- [14] M. Ahmad, A.U. Rajapaksha, J.E. Lim, M. Zhang, N. Bolan, D. Mohan, M. Vithanage, S.S. Lee, Y.S. Ok, Biochar as a sorbent for contaminant management in soil and water: a review, *Chemosphere*, 99 (2014) 19–33.
- [15] G.T. Li, X. Chen, L.Y. Xu, P.C. Lei, S. Zhang, C. Yang, Q.Y. Xiao, W.G. Zhao, Sonocatalytic degradation of methylene blue using biochars derived from sugarcane bagasse, *Desal. Water Treat.*, 88 (2017) 122–127.
- [16] S. Nikolaou, J. Vakrosa, E. Diamadopoulou, D. Mantzavinos, Sonochemical degradation of propylparaben in the presence of agro-industrial biochar, *J. Environ. Chem. Eng.*, 8 (2020) 104010, doi: 10.1016/j.jece.2020.104010.
- [17] J. Chu, J. Kang, S. Park, C. Lee, Enhanced sonocatalytic degradation of bisphenol A with a magnetically recoverable biochar composite using rice husk and rice bran as substrate, *J. Environ. Chem. Eng.*, 9 (2021) 105284, doi: 10.1016/j.jece.2021.105284.
- [18] B. Jun, Y. Kim, Y. Yoon, Y. Yea, C.M. Park, Enhanced sonocatalytic degradation of recalcitrant organic contaminants using a magnetically recoverable Ag/Fe-loaded activated biochar composite, *Ceram. Int.*, 46 (2020) 22521–22531.
- [19] D.P. Li, J.H. Qu, Research and technological development trends on drinking water safety assurance: water purification technologies based on interfacial interactions, *Chin. J. Environ. Eng.*, 4 (2010) 1921–1925 (in Chinese).
- [20] N. Kishimoto, S. Hamamoto, Removal of linear alkylbenzene sulfonate (LAS) by a cetyltrimethylammonium bromide (CTAB)-aided coagulation-filtration process, *Environ. Technol.*, 43 (2020) 815–823.
- [21] S. Ghosh, O. Falyouna, A. Malloum, A. Othmani, C. Bornman, H. Bedair, H. Onyeak, Z.T. Al-Sharif, A.O. Jacob, T. Miri, C. Osagie, S. Ahmadi, A general review on the use of advance oxidation and adsorption processes for the removal of furfural from industrial effluents, *Microporous Mesoporous Mater.*, 331 (2022) 111638, doi: 10.1016/j.micromeso.2021.111638.
- [22] I.P. Meneses, S.D. Novaes, R.S. Dezotti, P.V. Oliveira, D.F.S. Petri, CTAB-modified carboxymethyl cellulose/bagasse cryogels for the efficient removal of bisphenol A, methylene blue and Cr(VI) ions: batch and column adsorption studies, *J. Hazard. Mater.*, 421 (2022) 126804, doi: 10.1016/j.jhazmat.2021.126804.
- [23] F. Wang, D. Liu, P.W. Zheng, X.F. Ma, Synthesis of rectorite/Fe<sub>3</sub>O<sub>4</sub>-CTAB composite for the removal of nitrate and phosphate from water, *J. Ind. Eng. Chem.*, 41 (2016) 165–174.
- [24] G.E. Do Nascimento, R.A. de Freitas, J.M. Rodríguez-Díaz, P.M. Da Silva, T.H. Napoleão, M.M.M.B. Duarte, Degradation of the residual textile mixture cetyltrimethylammonium bromide/remazol yellow gold RNL-150%/reactive blue BF-5G: evaluation photo-peroxidation and photo-Fenton processes in LED and UV-C photoreactors, *Environ. Sci. Pollut. Res.*, 28 (2021) 64630–64641.
- [25] G.T. Li, H.Y. Li, X. Mi, W.G. Zhao, Enhanced adsorption of Orange II on bagasse-derived biochar by direct addition of CTAB, *Korean J. Chem. Eng.*, 36 (2019) 1274–1280.
- [26] N.S. Al-Thabaiti, Q.A. AlSulami, Z. Khan, Role of ionic surfactants on the activation of K<sub>2</sub>S<sub>2</sub>O<sub>8</sub> for the advanced oxidation processes, *J. Mol. Liq.*, 369 (2023) 120837, doi: 10.1016/j.molliq.2022.120837.
- [27] G.T. Li, W.Y. Zhu, L.F. Zhu, X.Q. Chai, Effect of pyrolytic temperature on the adsorptive removal of p-benzoquinone, tetracycline, and polyvinyl alcohol by the biochars from sugarcane bagasse, *Korean J. Chem. Eng.*, 33 (2016) 215–221.
- [28] J. Bandara, J.A. Mielczarski, J. Kiwi, Molecular mechanism of surface recognition. Azo dyes degradation on Fe, Ti, and Al oxides through metal sulfonate complexes, *Langmuir*, 15 (1999) 7670–7679.
- [29] Y. Jiang, C. Petrier, T.D. Waite, Kinetics and mechanisms of ultrasonic degradation of volatile chlorinated aromatics in aqueous solutions, *Ultrason. Sonochem.*, 9 (2002) 317–323.
- [30] N.N. Mahamuni, A.B. Pandit, Effect of additives on ultrasonic degradation of phenol, *Ultrason. Sonochem.*, 13 (2006) 165–174.
- [31] I.K. Konstantinou, T.A. Albanis, TiO<sub>2</sub>-assisted photocatalytic degradation of azo dyes in aqueous solution: kinetic and mechanistic investigations A review, *Appl. Catal., B*, 49 (2004) 1–14.
- [32] Y. Sun, J.J. Pignatello, Evidence for a surface dual hole-radical mechanism in the titanium dioxide photocatalytic oxidation of 2,4-D, *Environ. Sci. Technol.*, 29 (1995) 2065–2072.
- [33] G.T. Li, K.H. Wong, X.W. Zhang, C. Hu, J.C. Yu, R.C.Y. Chan, P.K. Wong, Degradation of AO7 using magnetic AgBr under visible light: the roles of oxidizing species, *Chemosphere*, 76 (2009) 1185–1191.
- [34] G.T. Li, W.G. Zhao, B.B. Wang, Q.Y. Gu, X.W. Zhang, Synergetic degradation of Acid Orange 7 by fly ash under ultrasonic irradiation, *Desal. Water Treat.*, 57 (2016) 2167–2174.
- [35] M. Styliadi, D.I. Kondarides, X.E. Verykios, Pathways of solar light-induced photocatalytic degradation of azo dyes in aqueous TiO<sub>2</sub> suspensions, *Appl. Catal., B*, 40 (2003) 271–286.
- [36] E. Manousaki, E. Psillakis, N. Kalogerakis, D. Mantzavinos, Degradation of sodium dodecylbenzene sulfonate in water by ultrasonic irradiation, *Water Res.*, 38 (2014) 3751–3759.
- [37] D.G. Wayment, D.J. Casadonte Jr., Frequency effect on the sonochemical remediation of alachlor, *Ultrason. Sonochem.*, 9 (2002) 251–257.
- [38] A.D. Gupta, H. Singh, S. Varjani, M.K. Awasthi, B.S. Giri, A. Pandey, A critical review on biochar-based catalysts for the abatement of toxic pollutants from water via advanced oxidation processes (AOPs), *Sci. Total Environ.*, 849 (2022) 157831, doi: 10.1016/j.scitotenv.2022.157831.
- [39] X.D. Zhu, Y.C. Liu, C. Zhou, G. Luo, S.C. Zhang, J.M. Chen, A novel porous carbon derived from hydrothermal carbon for efficient adsorption of tetracycline, *Carbon*, 77 (2014) 627–636.
- [40] W.T. Liu, D.J. Ren, J. Wu, Z.B. Wang, S.Q. Zhang, X.Q. Zhang, X.Y. Gong, Adsorption behavior of 2,4-DCP by rice straw biochar modified with CTAB, *Environ. Technol.*, 42 (2021) 3797–3806.
- [41] S. Chatterjee, M.W. Lee, S.H. Woo, Influence of impregnation of chitosan beads with cetyltrimethyl ammonium bromide on their structure and adsorption of Congo red from aqueous solutions, *Chem. Eng. J.*, 155 (2009) 254–259.
- [42] Z.X. Hua, Y.P. Pan, Q.K. Hong, Adsorption of Congo red dye in water by orange peel biochar modified with CTAB, *RSC Adv.*, 13 (2023) 12502–12508.